Computational Methodology For Resonant Nano-Plasma Theranostics For Cancer Treatment

A Pradhan[1], Y Yu*[2], S Nahar[1], E Silver[3], R Pitzer[1]
(1) The Ohio State University, Columbus, OH
(2) Thomas Jefferson University Hospital, Philadelphia, PA
(3) Harvard University, Cambridge, MA

We describe a program of computational nanospectroscopy to employ the atomic, molecular, and plasma physics of atomic resonance formation and subsequent Auger fluorescence processes of electron ejection and photon emission for in vivo diagnostics and therapy of cancerous tumors. The methodology relies of large-scale atomic computations and modeling to predict the positions and strengths of resonance features in heavy high-Z elements such as Platinum and Gold delived to tumor sites as nanoparticles. These resonance features can be targeted via X-ray absorption, followed by many pathways for the breakup of the resultant Auger processes. The theoretical computations will help guide mono-energtic X-ray sources, such as the Electron-Beam-Ion-Traps, to target resonance complexes in specific energy ranges, and thereby induce in situ secondary
(a) electron ejecion via autoionization leading to DNA strand breakups, and
(b) X-ray emission, both predominatly localized at the tumor site.
The methodology entails: (I) Large-scale computations for resonance complexes in high-Z nanoparticle elements or molecular compounds using the powerful Relatvistic R-matrix and the COLUMBUS packages of codes from quantum chemistry, and (II) Modeling of nano-plasma opacities, attenuation coefficients, and numerical simulation of spectral features, to support an integrated system for Resonant Nano-Plasma Theranostics for potential cancer diagnostics and therapy

NOTES:

We describe a computational scheme to model atomic resonances in high-Z nanoparticle plasmas for in vivo theranostics of cancerous tumors. The basic principles refer to: (a) Giant resonance complexes due to inner-shell electronic transitions (Nahar and Pradhan 2004, and references therein), (b) Auger decay and resonances yielding multiple secondary electron and photon emission (C. Le Sech 2000, Kobayashi 2003), and (c) Electron attachment and radiatively induced DNA strand breakups in malignant tumor cells in situ (Boudaiffa etal. 2000). The largest resonances arise simply from strong dipole transition arrays associated with 1s-2p (K), 2p-3d (L), 3d-4f (M) complexes, which contain up to many thousands of lines concentrated in specific energy ranges. Spectroscopic targeting of these resonances would subsequently lead to Auger fluorescence involving ionization and recombination of multiple ionization states of heavy ions on extremely short time-scales, from pico-second (10^{-12}s) to femto-second (10^{-15}s). K-shell resonance targeting may be achieved for high-Z species by X-rays in the tens of KeV range, high enough in energy to be comparable to conventional X-ray imaging regime. But resonant K-ionization would then trigger localized L-shell Auger emission of secondary electrons and photons (see Fig. 1a). This has two effects: (a) low-energy electrons initiate resonant formation of DNA strand breaks, and (b) induce DNA strand breakup by photoabsorption (for example, in Cyclo-Pt bound to plasmid DNA). Moreover, it has been shown that in vivo X-ray irradiation of gold nanoparticles embedded in cancerous tumors in mice leads to significant reduction in their sizes (Hainfeld etal. 2004). Unlike previous studies however, we exploit the new concept of resonant spectroscopy which should result in a large reduction in administered radiation dose except at the high-Z uptake site.

We can summarize our computational estimates for resonant diagnostics and therapy as follows. The near-resonance enhancement, relative to off-resonance, should be a factor of 11.6 for K-shell resonances, and a factor of 1200 for the huge L-shell resonance arrays. It needs emphasis that these resonances are NOT at the K- and L-shell ionization edges, as previous investigations assumed. In fact they are generally spread over a narrow energy range of up to 0.5 keV, close to but significantly away from, the edge energies. The spread of ~0.5 keV refers to multiple ionization stages of the element undergoing Auger ionization. As described earlier, since K-shell ionization energies of high-Z elements such as gold are ~80 keV with long attenuation lengths of up to 20 cm, K-shell resonant absorption by nanoparticles attached to tumors could serve as diagnostics (using sensitive detectors). Resultant L-shell fluorescent emission due to Auger decay would be localized, owing to its short attenuation of < 1 cm, and should serve as therapy components (Fig. 1b).

The basic methodology entails targeting K-resonance complexes with trapping of resultant fluorescent radiative decays from L- and M-shells, and electron cascades from multiple ionization stages. It is important to note that the in situ production of secondary low-energy electrons by Auger ionization would also induce DNA strand breakup via electron attachment resonances (Boudaiffa 2000). Therefore resonance fluorescence yields two exactly complementary branches of photon emission and electron ejection for in vivo theranostics. The relative rates for the two branches vary from neutral to highly ionized (few-electron) stages: For neutral atoms, initially in molecular formations with approximate bond breakup energies of the order of tens of eV, creation of K-shell vacancies would lead primarily to L → K fluorescent X-ray emission nearly matching the incident energies of about ~80 keV in gold or platinum (modulated by the local environment or density contrast). But as fluorescent emission is isotropic, much of this high-energy radiation would be directed (a) within the tumor, and (b) to further ionization of other nanoparticles. Subsequent L → M cascades, and electron ejections due to these ìhollowî atoms also result and have been extensively studied in laboratory experiments. At the opposite end of ionization, highly ionized atoms divide almost equally between Auger electron ejection and photon emission with rates of both processes of about $10^{13\text{-}14}$/sec in high-Z ions. So the ratio of photo/electron production ranges from nearly 1 to ~0.5 from resonant complexes.

However, since the resultant products of resonant complexes in nano-plasmoids would be trapped inside the tumor (as desired), it is essential to model a priori, and calibrate against EBIT experiments, the full spectrum of photon and electron energies and fluxes. Initially such experiments and calibration would be carried out in vitro. For example, we shall first study relatively lighter-Z compounds of bromine and iodine, Bromodeoxyuridine (BUdR) and Iodeoxyuridine (IUdR), injected directly into the tissue. Later experiments would calibrate the high-Z compounds such as platinum in cis-Pt or gold nanoparticles.

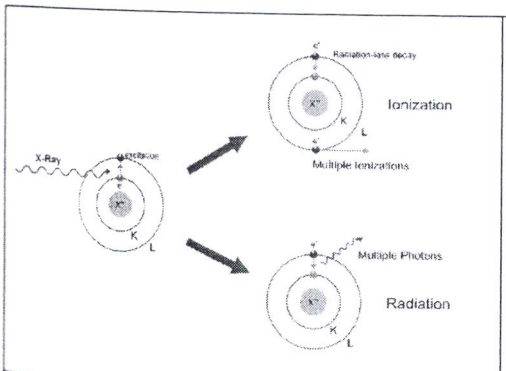

Fig. 1a. Schematic diagram of autoionization and radiative decay.

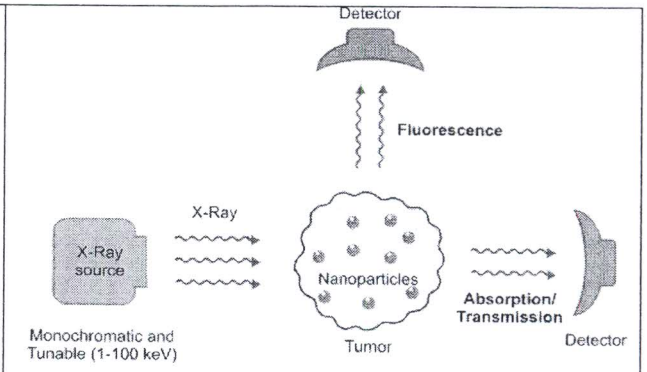

Fig. 1b. Schematic components of the proposed system.

K-shell emission X-ray will be used for diagnostic imaging, and L-shell emission X-ray will be used for therapy. This is because more energetic resonance emission photons can more readily escape from tissue without interaction, thus carrying intact spectroscopic fingerprints to the detector, whereas low energy resonance emission photons will deposit dose locally at the interaction site. For example, gold has K-shell emissions near 80 keV, and L-shell emissions near 12 keV, suitably matching the imaging and therapy requirements, respectively. The shape of the resonance profile, its magnitude and lifetime will be predicted to a fundamental level of accuracy by the computational core of this program for atoms and ions of interest (including metals used by published nano-biotechnology studies).

The spectral features in moderately heavy elements such as iron appear at energies E >1 keV, where the lighter biogenic elements H, C, N, and O are no longer effective absorbers of X-rays. For example, there are no resonances in oxygen above ~ 0.7 keV, and the absorption cross section behaves as the dashed line in Fig. 2. Our recent calculations for neutral oxygen show that the largest resonance is at 0.53 keV (Pradhan 2003).

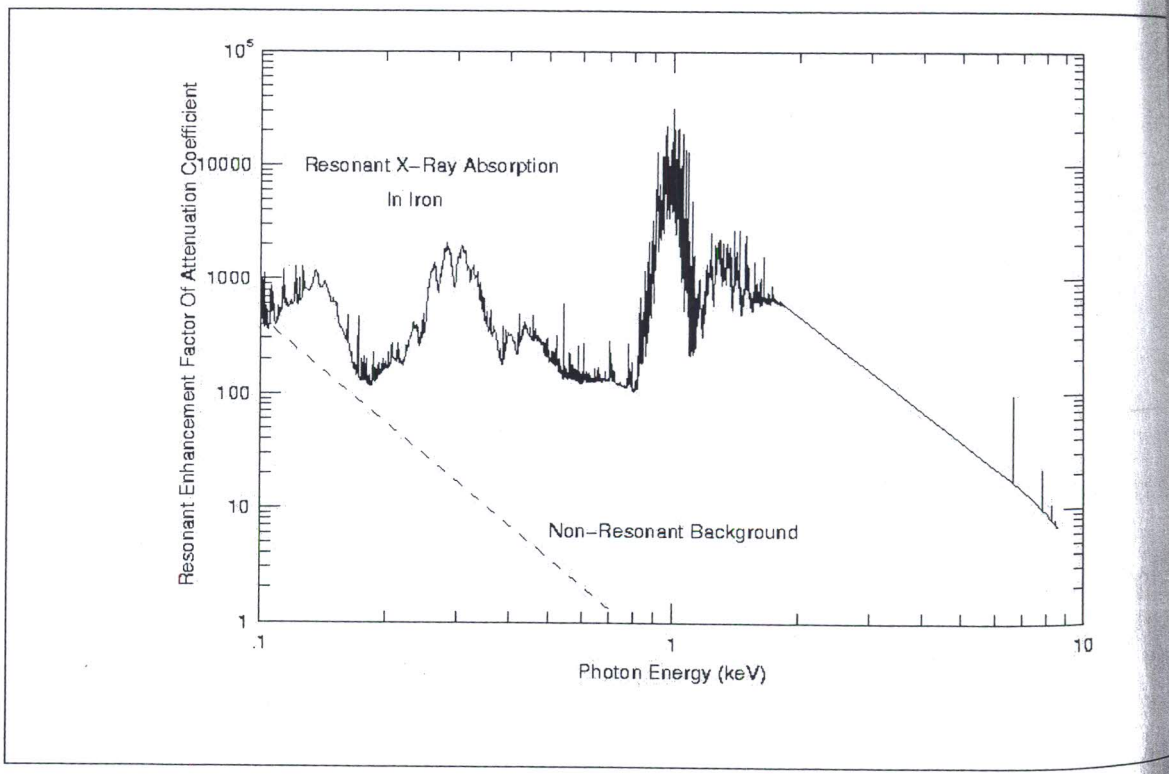

Fig. 2. Resonant spectroscopic signatures in iron. X-ray photoabsorption attenuation coefficient may be enhanced by up to orders of magnitude at specific spectral windows, such as the 1 keV L-shell resonance complex mainly due to strong 2p-3d dipole transition arrays. Biogenic elements H, C, N, and O do not absorb X-rays resonantly at these high energies. Significantly heavier elements than the iron group would be efficient absorbers / emitters at E >>10 keV for reduced tissue attenuation. All ionization stages of iron from neutral to highly charged, with only a few electrons in the L-shell, contribute to the 1 keV resonance feature, depending on the temperature and density prevailing in the ionized plasma environment.

The modeling component of the proposed program is based on the Relativistic R-matrix method, complemented by molecular structure calculations from the COLUMBUS package of codes. Numerical simulations for high-Z nanoparticles are computationally very involved. We plan to provide:

Detailed theoretical spectra of potential nanoparticle compounds with medium- to high-Z elements such as Bromine, Iodine, Palladium, Platinum, and Gold;

Precise estimates of the positions and strengths of resonance complexes;

Build a database of attenuation coefficients including all resonant and non-resonant processes.

Explore the efficacy of multiple-Z nanoparticles whereby the L-shell emission from a higher-Z element might match the K-shell absorption of a lighter-Z species.

LITERATURE CITED

Boudaiffa, B., Cloutier, P., Hunting, D.J., Huels, M.A. et Sanche, L., Science 287, 1658-1660 (2000).

J.F. Hainfeld, D.N. Slatkin, and H.N. Smilowitz, Phys. Med. Biol. 49, N309 (2004).

Seaton, M.J., Yu, Y., Mihalas, D., Pradhan, A.K. (1994). *Mon. Not. Royal Astron. Soc.* **266** 805,

Nahar, S.N., and Pradhan, A.K., in Radiation Physics and Chemistry 70, 323-344, Elsevier (2004).

Pradhan, A.K., Chen, G.-X., Delahaye, F., Nahar, S.N. and Oelgoetz, J., Mon. Not. Roy. Astr. Soc., 341, 1268 (2003).

C. Le Sech, K. Takakura, C. Saint-Marc, H. Forhlich, M. Charlier, N. Usami and K. Kobayashi, Radiat. Res. 153, 454-458 (2000).

K. Kobayashi, N. Usami, I. Sasaki, H. Frohlich, C. Le Sech, Nucl. Inst. and Meth. in Phys. Res. B (NIMB), 199, 348-355 (2003).